Expanded specific T cells to hypomutated regions of the SARS-CoV-2 using mRNA electroporated antigen-presenting cells

Elizabeth Ogando-Rivas,[1,3] Paul Castillo,[2,3] Changlin Yang,[1] Vrunda Trivedi,[1] Dingpeng Zhang,[1] Fernanda Pohl-Guimarães,[1] Ruixuan Liu,[1] Arnav Barpujari,[2] Kate M. Candelario,[1] Hector Mendez-Gomez,[1] Elias J. Sayour,[1,2] and Duane A. Mitchell[1]

[1]UF Brain Tumor Immunotherapy Program, Preston A. Wells Center for Brain Tumor Therapy, Lillian S. Wells Department of Neurosurgery, University of Florida, Gainesville, FL, USA; [2]UF Division of Pediatric Hematology Oncology, Department of Pediatrics, University of Florida, Gainesville, FL, USA

The COVID-19 pandemic has caused about seven million deaths worldwide. Preventative vaccines have been developed including Spike gp mRNA-based vaccines that provide protection to immunocompetent patients. However, patients with primary immunodeficiencies, patients with cancer, or hematopoietic stem cell transplant recipients are not able to mount robust immune responses against current vaccine approaches. We propose to target structural SARS-CoV-2 antigens (i.e., Spike gp, Membrane, Nucleocapsid, and Envelope) using circulating human antigen-presenting cells electroporated with full length SARS-CoV-2 structural protein-encoding mRNAs to activate and expand specific T cells. Based on the Th1-type cytokine and cytolytic enzyme secretion upon antigen rechallenge, we were able to generate SARS-CoV-2 specific T cells in up to 70% of unexposed unvaccinated healthy donors (HDs) after 3 subsequent stimulations and in 100% of recovered patients (RPs) after 2 stimulations. By means of SARS-CoV-2 specific TCRβ repertoire analysis, T cells specific to Spike gp-derived hypomutated regions were identified in HDs and RPs despite viral genomic evolution. Hence, we demonstrated that SARS-CoV-2 mRNA-loaded antigen-presenting cells are effective activating and expanding COVID19-specific T cells. This approach represents an alternative to patients who are not able to mount adaptive immune responses to current COVID-19 vaccines with potential protection across new variants that have conserved genetic regions.

INTRODUCTION

The world has experienced a devastating pandemic to which close to seven million lives have succumbed[1] and many others are dealing with long-term complications.[2,3] The novel coronavirus, SARS-CoV-2, was identified as the cause of the COVID-19 disease recognized as a pandemic by the World Health Organization (WHO) on March 11, 2020.[4] Up to March, 2023, COVID-19 has caused more than 675 million cases worldwide.[5] Unfortunately, these statistics will continue to increase due to the virus mutating into variants with higher ability of dissemination than the previous viruses and

with the potential risk of developing more deadly variants. The most clinically relevant variants so far described are the United Kingdom (alpha) variant 501Y.V1 lineage B.1.1.7[6]; the South Africa (beta) variant 501Y.V2 lineage B.1.351[6]; the Brazilian (gamma) variant 501Y.V3 lineage P.1[7]; the California variant CAL.20C lineages B.1.427–429[8]; the Indian (delta) variant S:478K lineage B.1.617.2[9]; and the omicron variants.[10]

To prevent further deaths and long-term disabilities, preventative vaccines have been developed including mRNA nanoparticle vaccines (Pfizer-BioNTech, Moderna), recombinant protein nanoparticle vaccine (Novavax),[11] non-replicating viral vector vaccine (Janssen, AstraZeneca, Sputnik and CanSino),[11–13] and more recently a recombinant protein sub-unit vaccine (Corbevax). The protection of these vaccines against the ancestral virus ranges from 65% to 96% in immunocompetent people however that is not the case in immunosuppressed patients.[14–17] Patients with primary immunodeficiencies, patients with cancers, or hematopoietic stem cell transplant recipients with dysfunctional adaptive immunity are not able to mount robust immune responses to current vaccine approaches.[18–22]

To provide an alternative for this population lacking adaptive immune responses to vaccines, we propose to target structural SARS-CoV-2 antigens with a novel mRNA-based technology to activate immune T cell responses. Our approach uses full length structural SARS-CoV-2 antigen encoding mRNAs electroporated into a pool of human antigen-presenting cells (APCs), derived from peripheral blood mononuclear cells (PBMCs), allowing these cells to process and present a broad array of antigens in a more
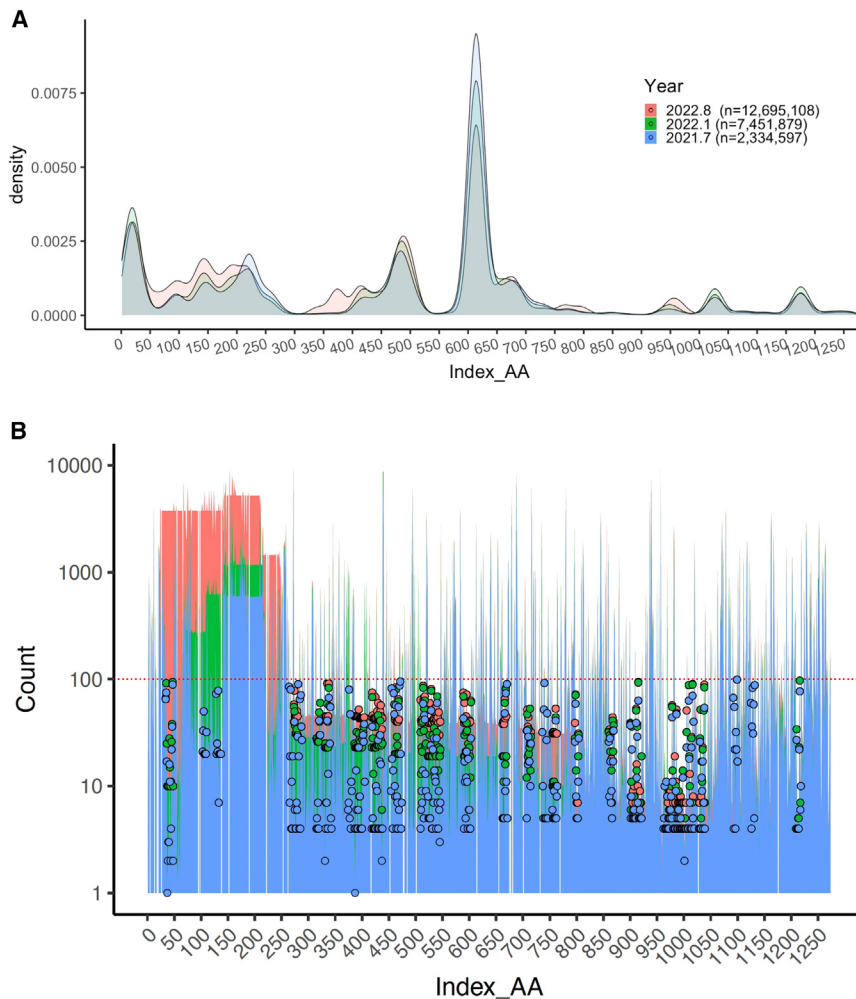
Figure 1. Evolution of Spike protein genome since the beginning of the COVID-19 pandemic

(A) density plot and (B) mutation count represent the mutational evolution of SARS-CoV-2 over 3 timepoints July 2021 (blue), January 2022 (green) and August 2022 (red). (A) Text boxes. represent the peaks of patient sample mutations corresponding to a different SARS-CoV-2 variant breakthrough. (B) Segmented red line represents the cut-off definition according to NCBI Virus by which at least 100 samples of different COVID-19 infected patients with the same mutation in the same position are considered single nucleotide variant (SNV). Thus, less than 100 samples with the same mutation in the same position at the amino acid level are defined as hypomutated regions in this study. Colored circles represent number of samples/patients with the same mutation that is below hypomutated region cut-off (segmented red line, <100 hits). Blue circles correspond to hypomutated regions for July 2021 period; green circles, hypomutated regions for January 2022; and red circles, conserved region for August 2022 time point.

Omicron variant later added more mutations which reduced number of hypomutated regions, from the period Dec 2019 to Jan 2022, as demonstrated by the red (August 2022, 2022.8) histogram. Next, the distribution of the Spike glycoprotein mutational count was plotted as histogram by time point (Figure 1B). We observed that the mutational count was markedly increased in broad regions across the first 800aa of Spike protein, however, the tail part of Spike protein rema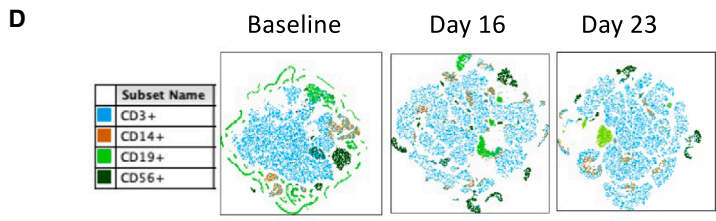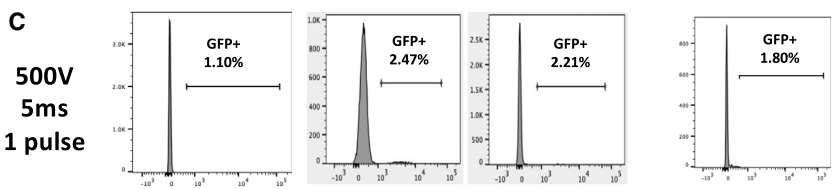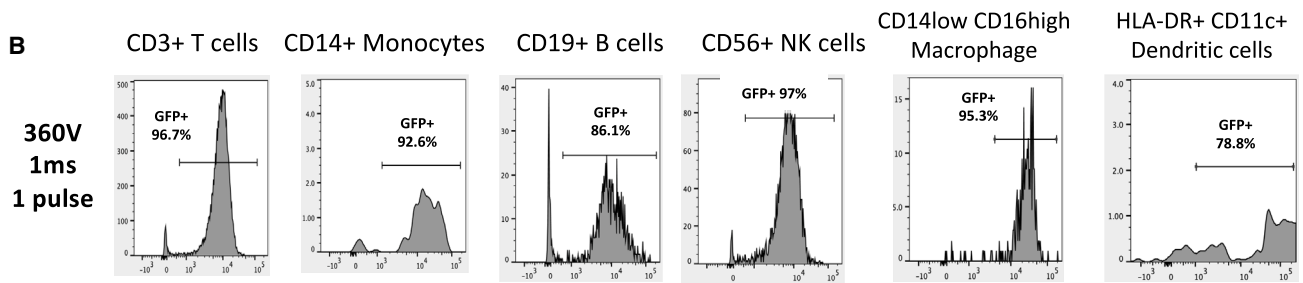ined most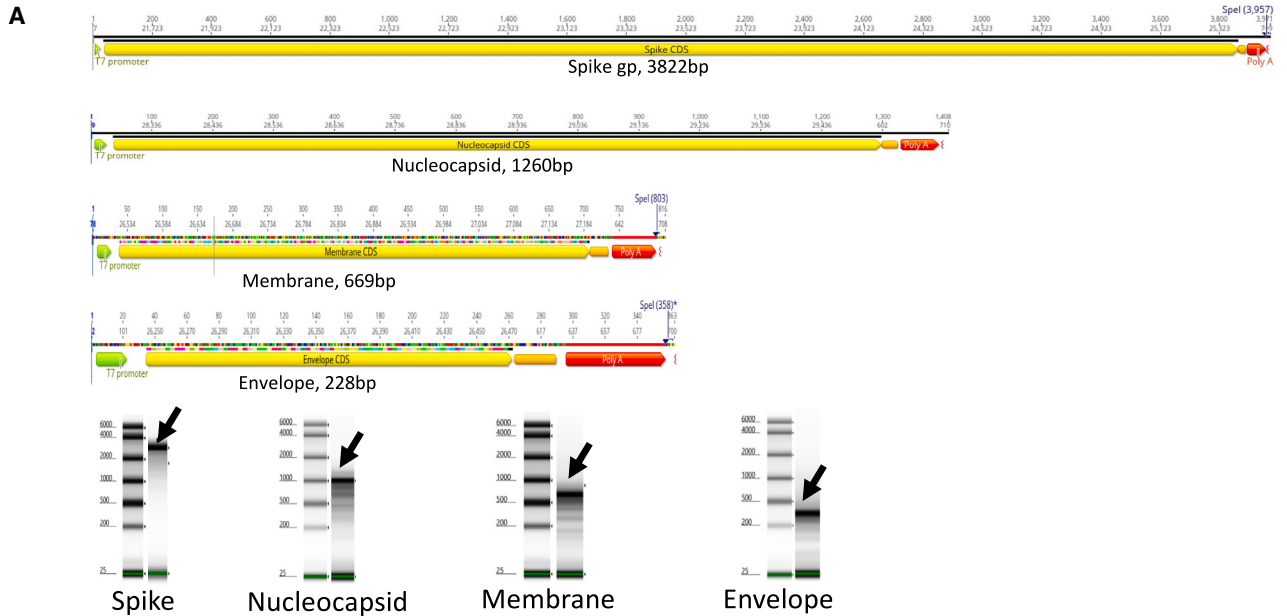ly conserved since Jul 2021 (Figures 1A and 1B). Hypomutated regions are illustrated by dots with different colors (blue, green, and red) corresponding to the surveyed years. Dots are the number of patients (less than 100 patients sharing the same point mutation in the same position at amino acid level, below segmented red line) that include regions of 8mers or more which were defined as hypomutated regions. Regions at the head and tail parts of Spike protein not showing red color dots indicate that those previously identified hypomutated regions were not detected in Aug 2022 due to the emergence of omicron variant with subsequent addition of more mutations. Hypomutations distributed from 250aa and 800aa presenting the three-color layers indicated that the mutation count of those regions increased as demonstrated by the higher overlap of Aug 2022 histogram and decreasing number of color dots for that same period. This suggests that hypomutations in this area are unstable. Favorably, hypomutations spanned from S:800aa to S:1050aa appear to be more stable as the overall number of patients with new mutations was lower compared with the S:250aa-800aa region (Figure 1B). Similar analyses for other SARS-CoV-2 structural antigens (Membrane, Nucleocapsid, and Envelope) are shown in Figure S1.

biological manner.[23–25] We showed feasibility of generating T cells specific to structural SARS-CoV-2 antigens and also to hypomutated regions conserved through the different viral variants. Thus, this approach can potentially confer protection to vulnerable patients infected with current or new variants that have conserved genetic regions.

RESULTS

Genomic evolution of SARS-CoV-2 and identification of hypomutated regions

We compiled a density plot and histogram to demonstrate the overall mutational changes from 2021 to 2022 in Spike gp amino acid sequence as proof of concept to demonstrate the mutational evolution of SARS-CoV-2. From July 2021 to January 2022, the variants of concern (VOCs) were alpha, beta, gamma, and delta. In January 2022, omicron variant emerged, and the mutational frequency started to accumulate in delta and omicron variants. We observed that Spike (S) regions between S:300-400aa, S:550aa, S:800-900aa, and S:1050-1150aa had low mutational frequency until January 2022 (2022.1) as depicted by the low mutational density histogram in Figure 1A.

A

Spike gp, 3822bp

Nucleocapsid, 1260bp

Membrane, 669bp

Envelope, 228bp

Spike   Nucleocapsid   Membrane   Envelope

B

CD3+ T cells   CD14+ Monocytes   CD19+ B cells   CD56+ NK cells   CD14low CD16high Macrophage   HLA-DR+ CD11c+ Dendritic cells

360V 1ms 1 pulse

GFP+ 96.7%   GFP+ 92.6%   GFP+ 86.1%   GFP+ 97%   GFP+ 95.3%   GFP+ 78.8%

C

500V 5ms 1 pulse

GFP+ 1.10%   GFP+ 2.47%   GFP+ 2.21%   GFP+ 1.80%

D

Baseline   Day 16   Day 23

Subset Name
CD3+
CD14+
CD19+
CD56+

(legend on next page)

Generation of SARS-CoV-2 antigen encoding mRNAs and feasibility of manufacturing SARS-CoV-2 RNA-based cellular therapy

We designed and generated messenger RNA constructs encoding for the full length of Spike, Membrane, Nucleocapsid and Envelop proteins (Figure 2A). The messenger RNAs obtained underwent quality control to determine that there was none to minimal degradation, truncated RNA bands, or cross-contamination of samples. We detected the electrophoresis bands and the corresponding RNA peaks in the expected position for the size of the construct (Figure 2A). These mRNAs were used to transduce whole human antigen-presenting cells (APCs) to expand SARS-CoV-2 antigen-specific T cells following the workflow depicted in **Graphical Abstract**. PBMCs were plated overnight for adherence activation and cells collected for electroporation.[26] To determine what immune cell populations were successfully electroporated, we initially electroporated PBMCs with two different settings of electroporation 360V 1ms 1 pulse and 500V 5ms 1 pulse with GFP mRNA. We then evaluated the GFP expression by NK cells (CD56$^+$), T cells (CD3$^+$), macrophages (CD14^{low} CD16^{high}), monocytes (CD14$^+$), B cells (CD19$^+$), and dendritic cells (HLA-DR$^+$ CD11c$^+$) by flow cytometry. For the 360V 1ms group, the GFP expression was 97%, 96.7%, 95%, 92.6%, 86.1%, and 78% for the different cell subtypes, respectively (Figures 2B and S3). For the 500V 5ms group, the GFP expression was <2.5% for all different cell subtypes (Figures 2C and S3). Thus, we proceeded with 360V 1ms for electroporation of PBMCs for all subsequent experiments. Next, we evaluated the cellular viability post-electroporation with Spike glycoprotein encoding mRNA at multiple time points. After 18 h post-electroporation, flow-cytometric evaluation showed between 87% and 97% viability of cell subtypes assessed (i.e., CD3 T cells, CD19 B cells, CD14 monocytes, and CD56 NK cells). After 42 h post-electroporation, the viability of unelectroporated cells versus electroporated cells was comparable (Table 1). Despite the known toxicity associated with electroporation, these findings suggest that our electroporation strategy maintains an acceptable cellular viability over time. As the culture progresses, the predominant cell population was CD3$^+$ T cells whereas the other cell subsets evaluated decreased over time suggesting expansion of antigen-specific T cells (Figure 2D).

Identification of SARS-CoV-2 structural antigen and hypomutated region-specific T cells

The T cells expanded with RNA-electroporated APCs were then evaluated for the presence of SARS-CoV-2 specific T cell receptors (TCRs). We interrogated the TCRβ repertoires of enrolled subjects to determine if all SARS-CoV-2 specific TCRβs and SARS-CoV-2 hypomutated region specific TCRβs were expanded to suggest cross-reactivity across ancient and emerging variants. At baseline, we observed that HDs and RPs had SARS-CoV-2 specific TCRβs which were overall further expanded upon T-APC stimulation. In the case of HDs, S and M specific TCRβs increased after T cell expansion however N and E TCRβs did not and actually N TCRβ repertoire shrunk. For RPs, specific TCRβs to all antigens (S, M, N, E) were expanded *in vitro* with the most robust findings observed in the case of S and N antigens (Figure 3A). Next, we screen for TCRβs specific to hypomutated regions. We found that only S protein retained immunogenic hypomutated antigens were markedly expanded in RPs compared with HDs (Figure 3B) using the SARS-CoV-2 genomic evolution time point of August 2022. The variability of TCRβs decreased upon stimulation with RNA-loaded APCs suggesting immune dominance of certain hypomutated regions with a more oligoclonal TCRβ expansion for RPs against hypomutated regions (Figures 3C and 3d). Upon evaluation of TCRβ usage, the dominant VDJ rearrangement was for HDs V04.01-J02.03 and RPs V07.08-J02.07. For RPs, the predominant VDJ rearrangement has been identified as one of the most common ones globally found in publicly available databases for patients diagnosed with COVID-19.[27]

Immune characterization of SARS-CoV-2 specific T cells

On day 0, PBMCs from HDs and RPs had similar frequency of CD3$^+$CD4$^+$ T cells (58.4%–81% vs. 71.8%–87.5%, p = 0.90) compared with similar trend but lower frequencies of CD3$^+$CD8$^+$ T cells (HD 19%–41.6% vs. RP 12.5%–28.2%, p = 0.90). However, it is until day 23 (after 3 stimulations) when HD CD3$^+$CD4$^+$ T cells were significantly lower than RP CD3$^+$CD4$^+$ T cells (p = 0.005). The opposite trend was observed for CD3$^+$CD8$^+$ T cells (p = 0.005). As the T cell culture progressed, the percentage of HD CD3$^+$CD4$^+$ T cells reduced and HD CD3$^+$CD8$^+$ T cells increased however maintaining CD3$^+$CD4$^+$ T cells predominance whereas the RP CD3$^+$CD4$^+$ and RP CD3$^+$CD8$^+$ T cell frequencies remain relatively stable (Figure 4A). To visualize the overall dynamic changes for maturation stages and checkpoint markers, we projected the global Spike gp-specific T cell differentiation patterns into the high-dimensional tSNE algorithm. Regarding T cell maturation, HD central memory (CM represented in blue) CD3$^+$CD4$^+$ T cell and CD3$^+$CD8$^+$ T cell frequencies did not change markedly between the three timepoints (Day 0, 16, and 23). However, for the RP (CM) CD3$^+$CD4$^+$ T cell and CD3$^+$CD8$^+$ T cell populations decreased dramatically, compared to their baseline. Regarding HD effector memory (EM represented in red) CD3$^+$CD4$^+$ T cells and CD3$^+$CD8$^+$ T cells slightly increased compared to their day 0 while RP (EM) CD3$^+$CD4$^+$ T cell and CD3$^+$CD8$^+$ T cell populations increased substantially (Figure 4B). For T cell checkpoint expression during cell culture, PD1 and Tim3 expression frequency on HD increased over time reaching their peak after 3 stimulations. However, in RPs PD1 and Tim3 expression frequency had a marked increase after 2 stimulations, particularly for CD3$^+$CD4$^+$ T cells (Figure 4B).

Figure 2. Generation of SARS-CoV-2 mRNAs for transfection of peripheral blood mononuclear cells

(A) represents plasmid constructs for Spike, Membrane, Nucleocapsid, and Envelope structural proteins and shows electrophoresis gels with RNA bands (black arrows) corresponding to Spike, Membrane, Nucleocapsid, and Envelope structural proteins. (B, and C) shows electroporation parameters and the type of cell subsets transduced. (D) Progression of cell subsets over the duration of cell culture for activation of antigen specific T cells.

Table 1. Viability over time of electroporated cells compared with unelectroporated cells

Timepoints	Unelectroporated	Electroporated
Trypan blue		
At 0 h	85%	85%
At 6 h	85%	81.4%
At 18 h	84%	83%
At 42 h	77%	85%
Flow cytometry		
At 18 h		
CD3	91.5%	87%
CD14	94%	94%
CD56	91%	92%
CD19	92%	91%

Viability was assessed by trypan blue counting and by flow cytometry using Zombie Violet live-dead staining.

We next compared the immune phenotyping of T cells specific against Spike and non-Spike structural antigens (M, N, and E) upon cognate peptide rechallenge. We perform flow cytometric analysis of the generated T cell subsets and compared their immune signature across all SARS-CoV-2 antigens using Day 16 as time point for all conditions. For HDs and RPs, the CM CD3$^+$CD4$^+$ and CD3$^+$CD8$^+$ T cells decreased or remain unchanged compared with unstimulated T cells upon SARS-CoV-2 structural peptide challenge. There was a clear increase in the overall EM populations compared with unstimulated T cells for all antigens (Figure S2). Checkpoint markers (i.e., PD1, Tim3, Lag3) were also measured as surrogate markers of activation. In HD CD4$^+$ S T cells, we observed upregulation of PD1, Tim3, and Lag3 (from mean 0.65%–0.82% to 7.85%–10.13%; 0.23%–0.38% to 1.08%–1.36%; 0.45%–0.6% to 4.56%–6.23%, respectively) on day 16 versus day 0. In the case of HD CD8$^+$ T cells on day 16, upregulation of PD1, Tim3, and Lag3 was higher (3.42%–3.44% to 24.7%–26%; 0.16% to 3.56%–5.85%; 2.61%–2.76% to 8.77%–10.11%, respectively) (Figure 4C). Overall, RP CD4$^+$ S T cells showed higher upregulation of PD1, Tim3, and Lag3 after 2 stimulations (from 0.96%–1.33% to 41.25%–45.64%; 0.5%–0.51% to 10.60%–11.33%; 0.9%–0.93% to 18.68%–21.92%, respectively) (Figure 4C). RP CD8$^+$ S T cells trended to a more robustly increase PD1, Tim3 and Lag3 (13.43%–13.15% to 45.58%–47.31%; 0.32%–0.8% to 19.05%–25.57%; 5.1%–6.4% to 19.59%–28.44%, respectively) (Figure 4C). Particularly, PD1 and Tim3 were significantly upregulated in RP compared with HD when T cells were challenged with Spike gp (p < 0.001 and p < 0.05, respectively) antigens whereas only PD1 was significantly increased in RP M T cells and RP N T cells compared with HDs (p < 0.005, both). Similar trends were observed for Membrane, Nucleocapsid and Envelope however with overall lower checkpoint expression level than for Spike gp. We also assessed whether IFNγ release correlated with checkpoint expression. We confirmed that increasing IFNγ secretion was associated with higher PD1 expression in HDs whereas decreasing IFNγ secretion happened in the setting of lower PD1 expression in RPs when comparing day 16 versus day 23 (Figure 4C).

Functionality and specificity of T cells

We tested specific T cell responses against all SARS-CoV-2 structural antigens. First, we assessed cell proliferation after two stimulations. By day 17, all donors (3 HDs and 3 RPs) had over 10-fold expansion (fold expansion range: 13.8–48.8) (Figure 5A). The remarkable T cell proliferation for all HDs supports the concept that SARS-CoV-2 unexposed unvaccinated HDs have memory T cell precursors likely from exposure to other coronaviruses. Next, we determined the overall trend of T cell responses to S antigens in HDs and RPs and their corresponding TCRβ clonality. TCRβ repertoire is depicted at baseline and after 2 or 3 stimulations for HDs and RPs based on the best IFNγ responses after antigen rechallenge (Figure 5B). For HD responders, the overall peak of IFNγ secretion was reached on day 23 (mean: 397.8 pg/mL; range: 71.4–613.83 pg/ml). For RPs, the IFNγ levels peaked on day 16 (mean: 2730.82 pg/mL; range: 1635.16–6796.27 pg/mL) and then decreased after 3 stimulations suggesting potential exhaustion of T cells (Figure 5B). These findings are likely related to the higher frequency of memory T cell precursors in RPs versus HDs. With subsequent stimulations, the SARS-CoV-2 TCRβ repertoire narrowed down which correlated with Simpson index closer to 1.0 suggesting exclusion of TCRβ not specific to SARS-CoV-2 (Figures 5B and 5C). The decreasing TCRβ repertoire over time indirectly correlated with IFNγ secretion levels likely associated with a robust expansion of SARS-CoV-2 specific T cells (Figure 5B).

SARS-CoV-2 specific T cells have a cytotoxic profile

Based on IFNγ secretion upon antigen rechallenge, we were able to generate S-specific T cells in 70% of HDs (n = 5 of 7) after 3 stimulations and in 100% of RPs (n = 8 of 8) after 2 stimulations when tracking individual responders (Figure 6A, and Table S1). Responders to M antigens were identified in 29% of HDs (mean: 1079.65 pg/mL; range: 901.41–1257.88 pg/mL) and 71% of RPs (mean: 1334.69 pg/mL; range: 1127.59–2080.23 pg/mL) whereas none of HDs and 57% of RPs (mean: 1575.78 pg/mL; range: 120.38–4128.18 pg/mL) were able to mount specific T cell responses to N antigens. For E antigens, we did not have responders among HDs however one RP (261.56 pg/mL) responded after 3 rounds of stimulation suggesting low immunogenicity from E protein (Figure 6A, and Table S1). Next, we evaluated granzyme B and perforin secretion of Spike gp-specific T cells that underwent 2 stimulations prior to rechallenge Spike gp peptides. For all donors tested (3 HDs and 3 RPs), there was increased antigen-specific secretion of granzyme B and perforin suggesting that the antigen-specific T cells are likely to not only recognize antigens specifically but also cytotoxic (Figure 6B).

To determine what T cell subsets secrete antigen-specific cytokines, intracellular staining for IFNγ, TNFα, and IL-2 was performed. Four donors, known to be Spike gp-specific responders, were evaluated. Products were chosen after 2nd or 3rd stimulation based on the time point with the peak of responses. Cytokine secretion patterns
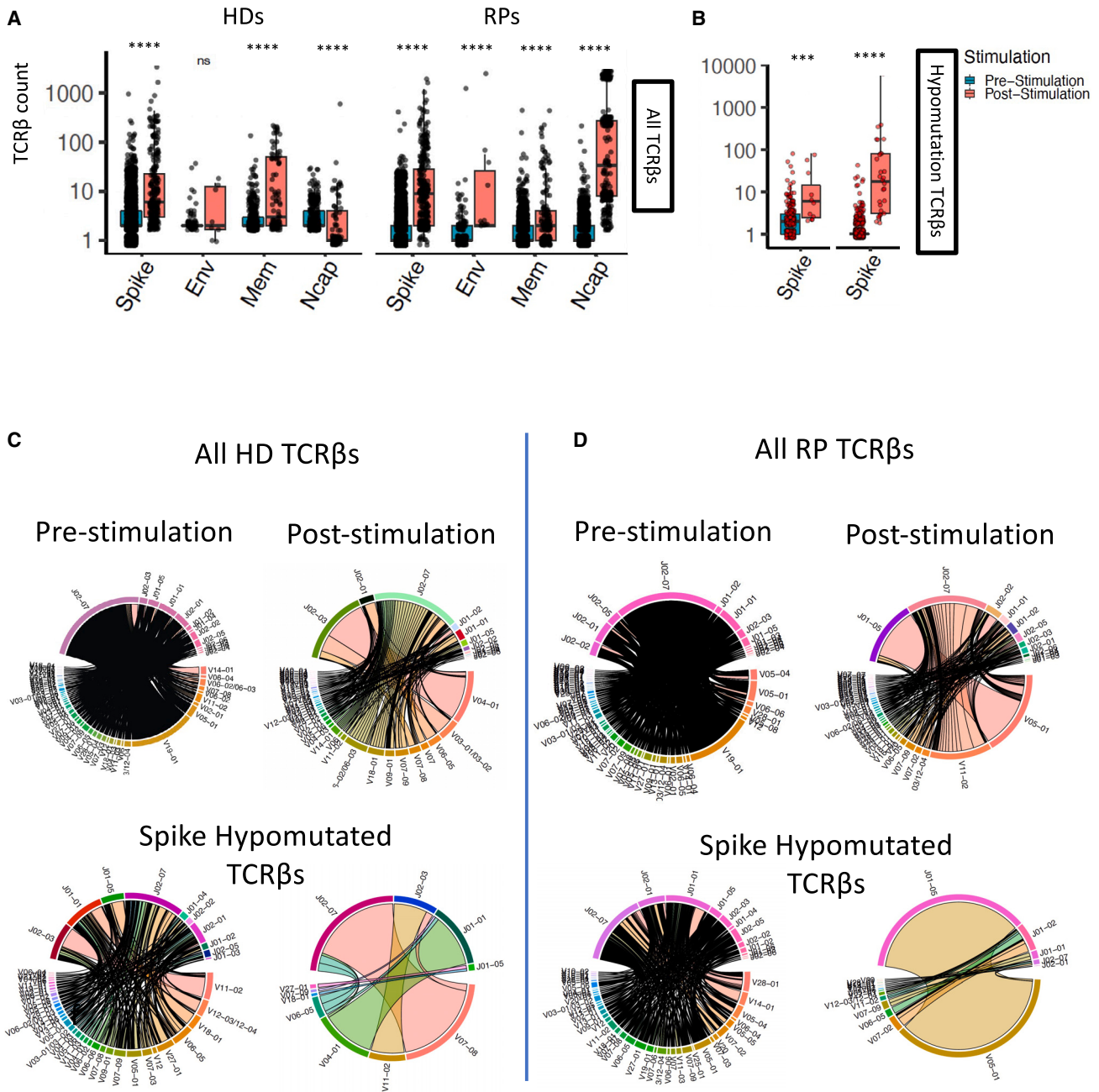
Figure 3. TCRβ count specific SARS-CoV-2 structural antigens
(A) TCRβs specific against SARS-CoV-2 antigens in healthy donors and recovered patients pre- and post-stimulation. (B) TCRβs specific to hypomutated regions pre- and post-stimulation. (C) Distribution of all TCRβs against SARSp-CoV-2 structural antigens (S, M, N, E) pre- and pos-stimulation in HDs. Distribution of Spike hypomutated region specific TCRβs pre- and post-stimulation in HDs. (D) Distribution of all TCRβs against SARSp-CoV-2 structural antigens (S, M, N, E) pre- and pos-stimulation in RPs. Distribution of Spike hypomutated region specific TCRβs pre- and post-stimulation in RPs.

were similar for CD3$^+$CD4$^+$ and CD3$^+$CD8$^+$ T cells with increased secretion of IFNγ and TNFα compared with unstimulated T cells (IFNγ mean: 10.7% vs. 2.3% CD3+CD4+ T cells & 12.4% vs. 2.6% CD3+CD8+ T cells; TNFα mean: 11.2% vs. 1.5% CD3+CD4+ T cells & 15% vs. 4.7% CD3+CD8+ T cells, respectively; p < 0.05)

and perhaps a trend toward increased IL-2 secretion in CD4+ T cells (Figures 6C, and S4).

We also wanted to determine if combining all 4 structural antigen-encoding mRNAs would provide similar high activation rates
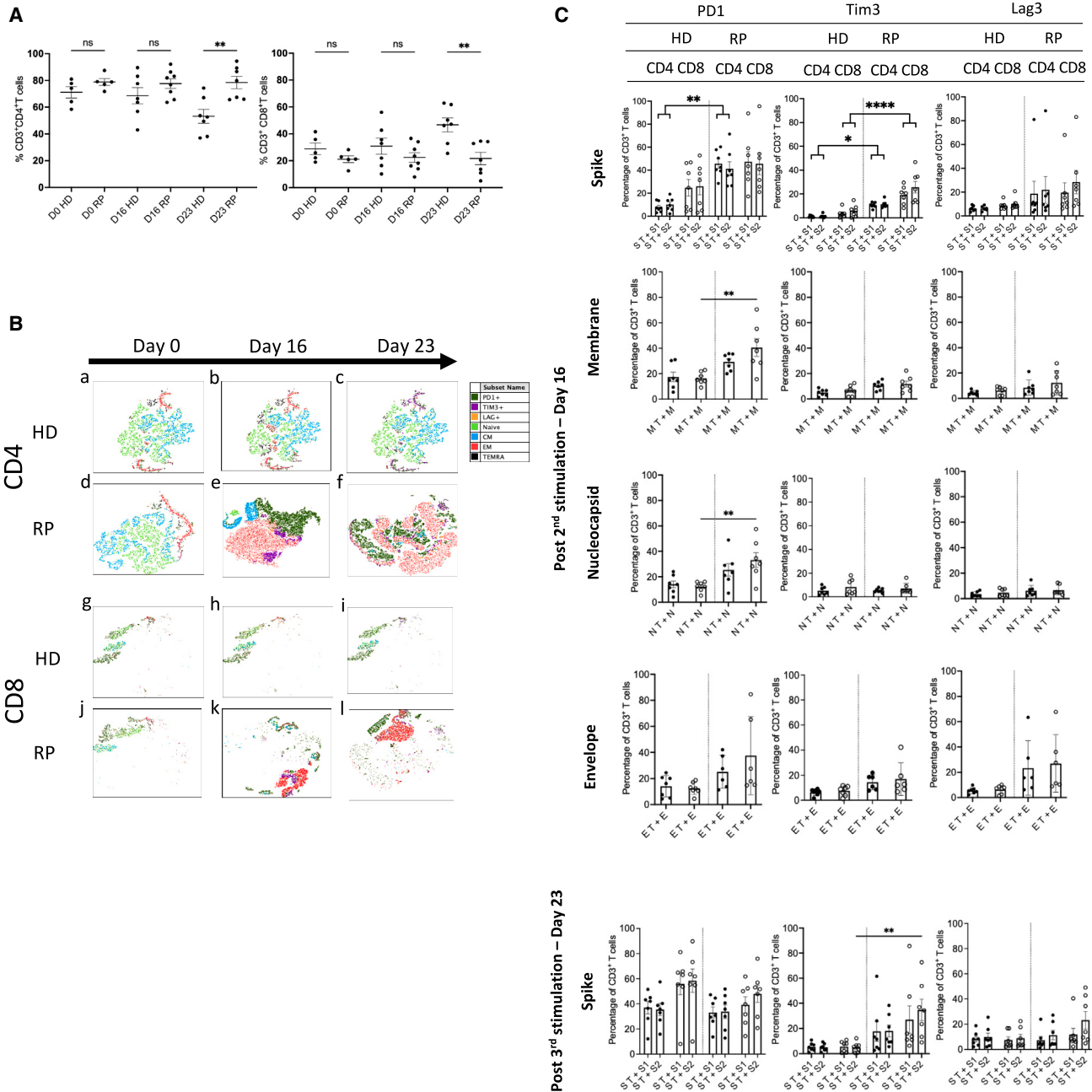
Figure 4. Immunophenotypic characterization of SARS-CoV-2 specific T cells

(A) CD3+CD4+ and CD3+CD8+ T cell distribution across HDs and RPs at baseline and over the course of cell culture. (B) tSNE representation of maturation stages (naive, central memory CM, effector memory EM, and TEMRA). (C) Checkpoint (PD1, Tim3, Lag3) immunophenotypic characterization across HDs and RPs and analysis across T cell subsets upon antigen challenge of activated T cells.

observed with single antigen mRNAs. HDs (n = 4) and RPs (n = 4) underwent 2 stimulations with all structural mRNAs simultaneously. 25% HDs and 75% RPs responded to at least one antigen, mainly Spike gp. The HD responder also had higher IFNγ levels to M and E antigens compared with controls. Among the RPs, one donor also had strong response to M and another donor had higher IFNγ to M, N, E antigens compared to controls (Figure S5). This lower yield of activation suggests the potential antigen predominance that polarizes response toward the immune dominant antigen. However, optimization of RNA concentration used during stimulations might also be needed to prevent skew of immune responses.
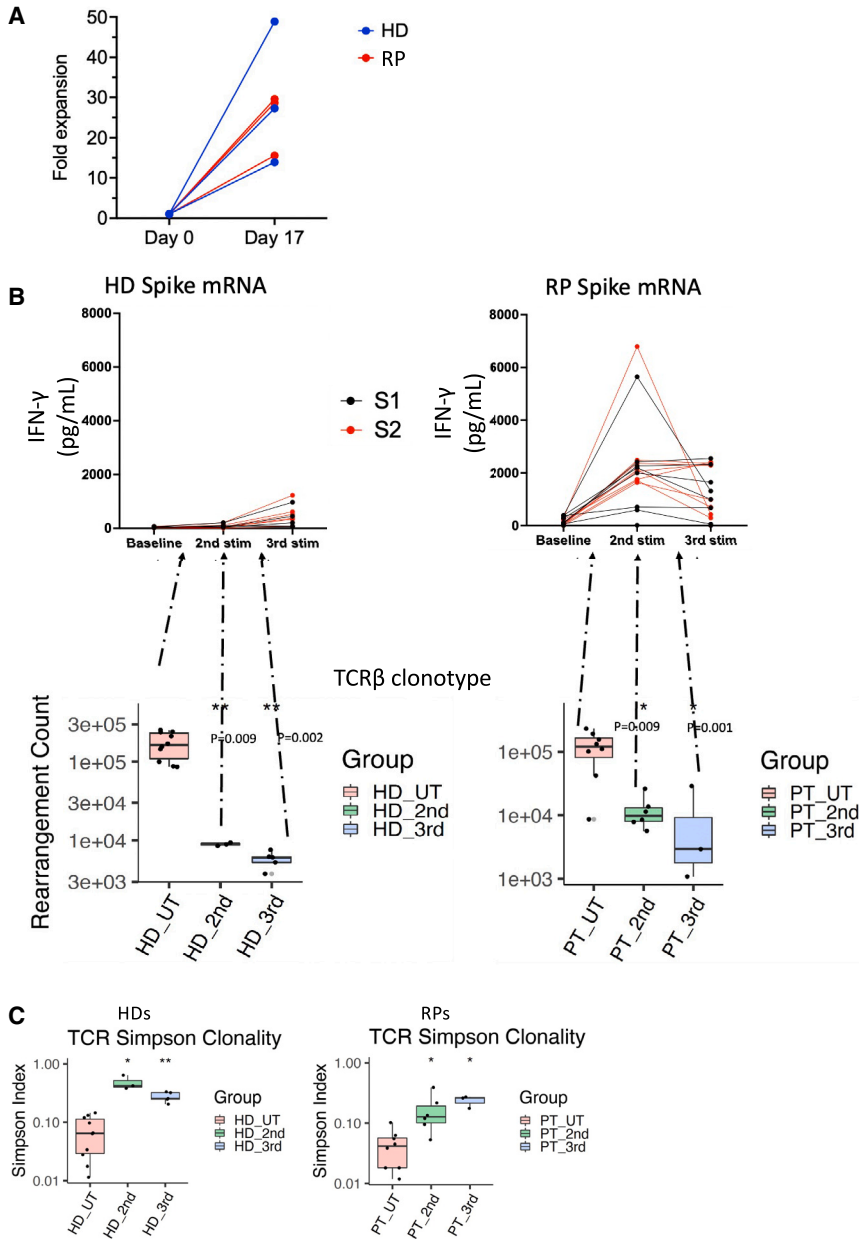
A

B

T cells specific against hypomutated and non-hypomutated regions of SARS-CoV-2 (Figure S6). Since the beginning of the pandemic, SARS-CoV-2 has genomically evolved with new variants acquiring mutations that confer increasing infectivity and virulence.[35] This mutational progression suggests the need for targeting conserved regions across ancient SARS-CoV-2 and its variants. We demonstrated that SARS-CoV-2 can conserve immunogenic antigens recognized by stimulated T cells from healthy donors and recovered patients. The demonstration that hypomutated regions evolve underscores the need for continuous genomic surveillance for preventative strategies for T cell immunity. These observations add to the current knowledge of adoptive T cell therapies against viral infections, that have classically used peptides to stimulate antigen specific T cells.

Efforts have started to address the gaps in the care of immunosuppressed patients and thus, SARS-CoV-2 peptide-based T cell therapies are being developed against structural SARS-CoV2 proteins.[36–38] Remarkably, we were able to mount T cell responses in about three-quarters of HDs, who were not previously exposed to COVID-19 or vaccinated against SARS-CoV2 immediately suggesting cross-reactivity with

C

DISCUSSION

The lack of effective preventive approaches for immunosuppressed patients, unable to mount humoral and/or cellular immunity to SARS-CoV-2, as well as the continuous evolution of variants that escape effective suppression by therapeutic monoclonal antibodies underscores the need to develop new technologies to provide protection against COVID-19 for this patient population. Our group has extensive experience developing RNA-based cellular therapies to expand T cells specific against virus-derived tumor antigens.[28–34] In this study, we use a novel approach that takes advantage of circulating APCs transfected with full-length SARS-CoV-2 structural protein encoding mRNAs to activate and expand low frequency

other types of coronaviruses. However, de novo priming and expansion of specific T cells cannot be excluded as a larger antigen repertoire may be presented by APCs loaded with full length mRNAs potentially due to a more physiologic antigen processing.[36,39–41] These observations support the notion that RNA-based therapies can be widely applicable and versatile approaches for adoptive T cell therapies.

We evaluated the mutational changes of SARS-CoV-2 Spike gp since the start of the pandemic given the relevance of this antigen as therapeutic target and we determined that hypomutated regions are still present within the SARS-CoV-2 genome. These hypomutated regions
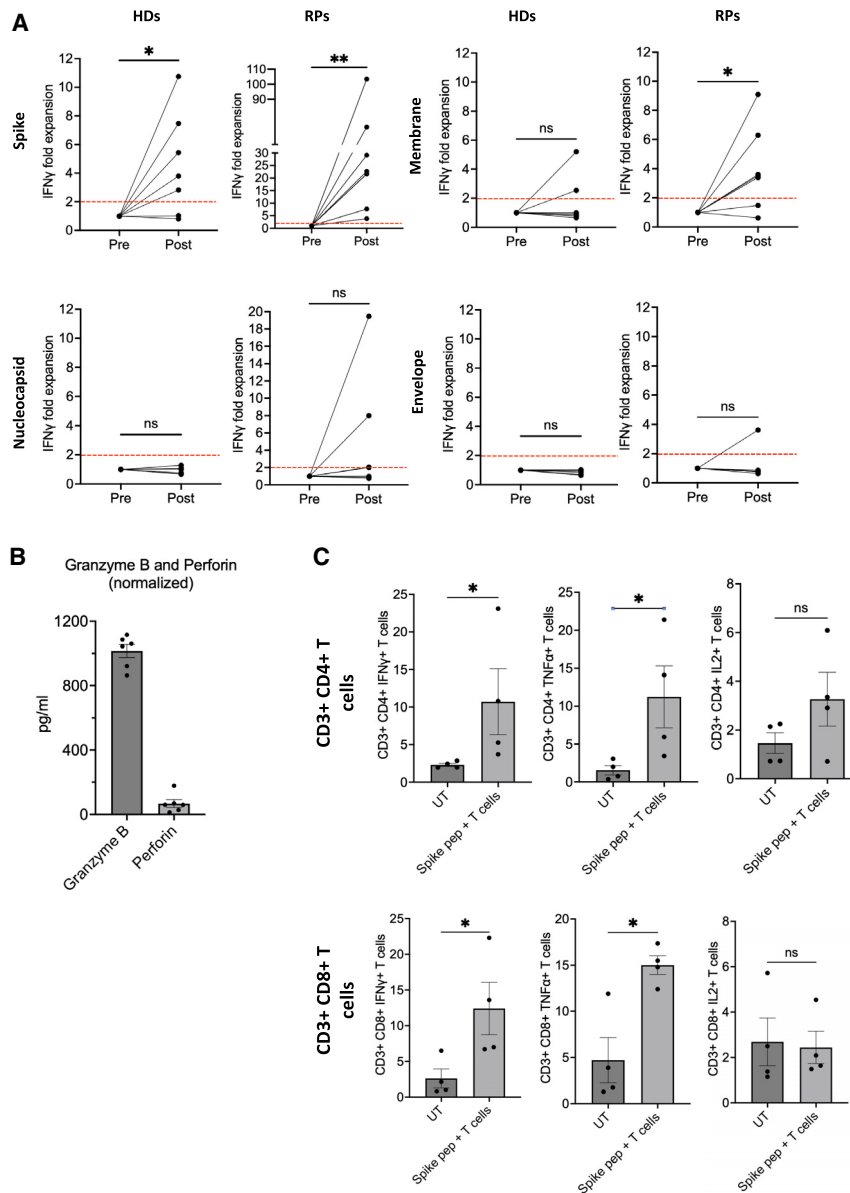
Figure 6. Cytotoxic profile of SARS-CoV-2 T cells

(A) IFNγ fold expansion are shown from T cells stimulated with all 4 structural protein encoding mRNA (spike, membrane, nucleocapsid, envelope). Red dotted line represents the cut-off to define responders (refer to materials and methods for definition). "Pre" indicates controls (i.e., unstimulated T cells, T cell alone, and T cell plus actin peptides). "Post" indicates SARS-CoV-2 stimulated T cells rechallenged with cognate peptides. (B) Granzyme B and perforin levels of T cells after two stimulations. Values were normalized by subtracting background control conditions. (C) Intracellular cytokine levels (i.e., IFNγ, TNFα, and IL-2) compared with untreated T cells (T cells alone). (*p < 0.05; **p < 0.001).

Groups have associated T cell activation status as potential contributing factors for severity of COVID-19 likely due to the lack of cellular protection.[42] In this study, we observed a marked increase of PD1, Tim3, and Lag3 expression after subsequent stimulations in CD3$^+$CD4$^+$ and CD3$^+$CD8$^+$ T cells preferentially against Spike protein. This pattern of checkpoint expression positively correlated with IFNγ secretion upon antigen rechallenge providing evidence that in some patients checkpoint expression might be a surrogate marker of outcomes for antiviral T cell response.

This approach represents an alternative to provide immunity to patients unable to mount clinically relevant anti-SARS-CoV-2 responses to current vaccines especially patients who are heavily immunosuppressed such as stem cell transplant patients, patients with immunodeficiencies or patients receiving B cell depleting agents such as anti-CD19 antibodies or CAR T cells. The presence of several TCRβ clonotypes capable of recognizing highly conserved regions has the promise of generating a therapeutic platform that can target current and potentially future variants. Furthermore, demonstration that hypomutated regions change overtime underscores the development of platforms that can be rapidly adapted through incorporation of antigen-encoding RNA matched to the evolving SARS-CoV-2 genome.

largely localized to Spike gp were immunogenic whereas other structural antigens have lost their conserved areas. It was previously shown that membrane protein contained immunogenic conserved regions however after evaluating the SARS-CoV-2 genome at the time of this study, those regions were lost according to our hypomutation selection criteria.[36] We identified up to 20 different hypomutated regions recognized by TCRβ clonotypes in HDs and RPs expanded against the ancient Spike gp encoding mRNA (Table S2). As expected, the TCRβ clones specific to those conserved regions were more robustly expanded in RPs versus HDs. Thus, the existing Spike gp hypomutated regions highlight the potential these regions have for developing adaptable and rapidly deployable platforms as preventative or therapeutic measures.

MATERIALS AND METHODS

Peripheral mononuclear cell (PBMCs) collection and isolation

We collected PBMCs from healthy donors (HDs) and recovered COVID-19 patients (RPs) after being consented by our local UF IRB protocol (IRB201701445). Of note, HDs were donors whose blood samples were drawn at the start of the pandemic, and they never had COVID-19 nor they were vaccinated. Seven HDs and eight RPs donated 60 mL of blood in sodium heparin tubes at 2 timepoints

separated by 4 weeks. The recovered patients who participated in this study where unvaccinated donors. PBMC layer was isolated by ficoll gradient centrifugation at 800g 15min and then either used fresh or frozen for downstream experiments.

Generation of SARS-CoV-2 spike gp (S), membrane (M), nucleocapsid (N) and Envelop (E) messenger RNAs (mRNAs)

To make SARS-CoV-2 Spike mRNA, Spike Coding Sequence (CDS) was extracted from plasmid (SinoBiological, VG40589-UT) using HindIII-HF and EcoRI-HF restriction enzymes (NEB, R3104S and R3101S, respectively). Subsequently, Spike CDS fragment was cloned into a modified pGEM4z (called pGEM4zR, Promega, P2161) plasmid that contains a T7 promoter and a 62 nucleotide long poly A sequence, creating pGEM4zR-Spike plasmid. To make Nucleocapsid mRNA, Nucleocapsid CDS from plasmid (Integrated DNA Technologies - IDT, 10006625) was amplified by PCR reaction and the fragment was cloned into pGEM4zR, creating pGEM4zR-Nucleocapsid plasmid. To make Membrane and Envelop mRNAs, CDS sequences were identified using SARS-CoV-2 genome (NCBI, MN908947), and these fragments were purchased from IDT and cloned into modified pGEM4z plasmid. All new constructs were fully sequenced (Azenta) to verify that full CDS was cloned, and mutations were not present. All pG4z plasmids were grown and opened with SpeI-HF restriction enzyme (NEB, R3133S). Opened plasmids were used as templates in *in vitro* RNA (IVT) reactions (Invitrogen, AM1344) to produce SARS-CoV-2 mRNAs. After IVT reactions, all mRNAs were purified using RNeasy Maxi Kits (Qiagen, 75162). mRNA concentration was measured by Nanodrop 2000c (ThermoFisher Scientific, ND-2000) and single mRNA specie purity was analyzed by using a bioanalyzer (Agilent, 2200 TapeStation System).

Generation of SARS-CoV-2 specific T cells

Upon isolation of PBMCs, fresh or frozen cells were used for generation of SARS-CoV-2 specific T cells. Frozen cells were thawed in 10mL of warm CTS Aim-V SFM (Gibco, FL) with 5% heated human AB serum (HS) (Valley Biomedical, VA) and rested overnight without cytokines to avoid non-specific growth of immune cells. PBMCs were plated in tissue culture treated 24-well plates in Aim-V without HS or cytokines at a cell density of $1x10^6$ PBMCs/ml. After 16–18 h (Day 0), non-adherent and adherent fractions were collected by mechanical harvesting. Next, bulk PBMCs were resuspended at a density of $2x10^6$-$5x10^6$ cells/200ul of OPTI-MEM (Life Technologies, CA) and mixed with 25ug COVID-19 antigen-encoding mRNA in 2mm electroporation cuvette (Fisher Scientific, MA). For multi-mRNA electroporation, 25ug of each structural antigen mRNAs were mixed in single suspension and used for downstream transfection. Cells were electroporated at 1 ms and 360 V using the ECM 830 BTX Electro Square Porator (Harvard Apparatus, MA). Electroporated PBMCs were plated in tissue culture treated 24-well place in recombinant human IL2 (50 U/ml)-containing Aim-V + 5% HS at a cell density of 1e6 PBMCs/ml per well. Over the following days, if cells were 100% confluent, cells were split and fresh IL2 containing culture medium was added. On day 9–10, the growing PBMCs were stimulated with

newly COVID-19 mRNA electroporated PBMCs, used as antigen-presenting cells (APCs), as aforementioned. To avoid non-specific cell growth, the new PBMCs were irradiated with 40Gy and co-culture with growing T cells at a ratio of 1:1. On day 16, a second stimulation was carried out. On day 23, cell culture was ended, and cells used for functional assays.

Functional assay

Restimulation functional assays were performed after 2nd and 3rd stimulations. Activated T cells were co-cultured with Spike gp (S1 and S2 subunits), Membrane, Nucleocapsid, and Envelope pepmixes (15 mer peptides with 11 overlapping amino acids spanning antigen peptide sequences) (JPT, Germany). Up to $5x10^5$ activated T cells were incubated with 0.2ug of corresponding pepmixes for 36 h in incubator at 37C and 5% CO_2. Supernatants were collected to evaluated for cytokines. Luminex-based cytokine bead array was performed by the Interdisciplinary Center for Biotechnology Research Proteomics Core. We defined responders when IFNg secretion level (in pg/ml) was at least double of the closest control (i.e., conditions containing unstimulated T cells co-cultured with SARS-CoV-2 pepmixes, T cells alone, or T cells co-cultured with actin pepmixes). T cells from this assay were also collected for flow analysis. To evaluate for granzyme B and perforin secretion, we followed same antigen rechallenge conditions for Spike gp-specific T cells. Supernatants were collected and used in an enzyme-linked immunosorbent assay (ELISA, Invitrogen, MA). For cases with high background, we normalized results by subtracting background from specific responses and then labeled "normalized".

Flow cytometry

For evaluation of GFP expression, anti-human CD3-APC, CD11c-BV711, CD14-APC, CD14-PE, CD16-APC, CD19-APC, CD56-APC and HLA-DR PE (BD Biosciences or BioLegend, CA). In a 96-well plate with $5x10^5$ cells per well (after antigen rechallenge per Functional Assay methodology), cells were washed with FACS buffer (phosphate buffered saline (PBS) + 2% of human AB serum) and stained with detection fluorochrome conjugated antibodies. For T cells, an 8-color panel including live/dead marker, propidium iodide, was used. These also included anti-human CD3-Qdot605, CD8-APC Cy7 and PD1-PE, Lag3- BV480, Tim3-VioBright FITC for checkpoint expression. To determine T-cell maturation staging staining was performed using anti-human CD62L-PE-dazzle and CD45RABV711. In this study, CD4 positive T cells were defined as the CD8 negative T cell populations. Cells were washed twice with FACS buffer before analysis via BD Symphony A3 at the Interdisciplinary Center for Biotechnology Research Flow Cytometry core. Further analysis was performed using tSNE (FlowJo).

For intracellular staining (ICS), anti-human CD3-Alexa Fluor 700, CD4-BV421, CD8-APC-H7, IFNγ-FITC, TNFα-APC, and IL-2-PE antibodies (BioLegend, CA) as well as brefeldin A, fixation buffer, and intracellular staining perm wash buffer (BioLegend, CA) were used. Manufacturer instructions for ICS were followed. Per functional assay methodology, T cells were stimulated with cognate antigens for

4 h. Then, 1X brefeldin A was added at a final concentration in cell culture of 10ug/ml for extra 4 h of incubation. Cell surface marker (CD3, CD4, and CD8) staining was performed at this point for 15–20 min at room temperature in the dark. Next, cells were centrifuged at 350g 5min. Cells were fixed with fixation buffer (0.5mL) for 20 min at room temperature and permeabilized 1X perm wash buffer (2mL, twice) followed by staining of intracellular markers (5ul per antibody) for 20 min at room temperature in the dark. After washing samples with perm wash buffer, samples were analyzed in BD Symphony A3 machine.

T cell receptor sequencing repertoire

Expanded T cells with SARS-CoV-2 antigen mRNAs at day 16 or 23 were collected for evaluation of T cell receptor beta (TCRβ) profile and their corresponding antigen recognition. TCRβ sequencing, determined by VDJ rearrangement that includes complementary-determining region 3 (CDR3) regions, has been previously performed using an unbiased multiplex PCR, of sorted activated T cells after stimulation with SARS-CoV-2 peptides (Multiplex Identification of T cell receptor Antigen Specificity, Adaptive Biotechnologies, WA). TCRβ sequences were mapped to structural antigens including Spike gp, Membrane, Nucleocapsid, Envelope, and ORFs (1ab, 3a, 6, 7a, 7b, 8, 10) (ImmuneCODE database, Adaptive Biotechnologies, WA).[43,44]

Bioinformatics platform and hypomutated regions

To evaluate SARS-CoV-2 genome, we used a publicly available source, GISAID (https://gisaid.org). We froze analysis on August 25th, 2022. All hypovariant mutations were called in 12,695,108 patients. Mutational density represents the proportion of patients with a given point mutation in relation to the total number of patients reported during the corresponding time point. We capture three different timepoints (July 2021, January 2022, August 2022) from this database. NCBI Virus shows, in Sequence Read Archive (SRA) records, that single nucleotide variants (SNVs) with at least 100 hits (100 samples) are selected as mutations of SARS-CoV-2 when compared with SARS-CoV-2 RefSeq, NC_045512.2 (https://www.ncbi.nlm.nih.gov/labs/virus/vssi/#/scov2_snp).[45] Thus, we defined the cut-off criteria for hypomutated regions as at least 100 hits (patients) harboring the most frequent same point mutation at the amino acid level in the same position, to be considered a true variant. SARS-CoV-2 protein fasta files were downloaded and processed on the University of Florida HiPerGator.[46,47] Briefly, all SARS-CoV-2 structural proteins (i.e., S, M, N, E) were extracted from raw fasta files. To calculate SARS-CoV-2 point mutation, only peptide lengths which were identical to Wuhan-Hu-1 were retained to downstream analysis. Sequences with ambiguous amino acids (X) were removed. Mutations were called by a customized python script which compared the difference between donor amino acid sequence and Wuhan-Hu-1 and populate the mutation frequency of each amino acid position. Since one single position may harbor different mutations (e.g., S: P9S 174 times, S: P9T 18 times, S: P9L 454 times), only the most abundant alterations of the same position were reported (e.g., position 9 with 454 mutations of the same type). Regions that reached 8mers or more within a given region in the SARS-CoV-2 genome that were present

in less than 100 donors were considered as hypomutated regions. Bed files were generated and used for protein extraction by getfasta bedtools.[48] cDNA sequences of hypomutated peptides were fetched from SARS-CoV-2 nucleotide sequence by an in-house bioinformatics analysis. Next, those nucleotide sequences were translated to peptides to examine the accuracy.

Statistical analysis

Seven healthy donors and eight recovered patients were analyzed statistically. Ordinary one-way ANOVA was used to make comparisons of flow cytometric parameters and cytokine release. Mean values are plotted with standard errors of the mean (SEM), unless otherwise stated in figure legends). In T-cell functional assays, donors were assessed as distinct technical duplicates and the average of those values were included in statistical analysis. For evaluation of TCR profiling, Wilcoxon signed ranked test for non-parametric data was used. Asterisks indicate level of significance ($p \geq 0.05$ not significant; $*p = 0.05$; $**p = 0.01$; $***p = 0.001$; $****p \leq 0.0001$). There were no statistical analyses used to predetermine sample size.

DATA AND CODE AVAILABILITY

Data available within the article and its supplemental materials. Coding script will be available upon reasonable request. Raw data will be available upon request to corresponding author (duane.mitchell@neurosurgery.ufl.edu).

SUPPLEMENTAL INFORMATION

Supplemental information can be found online at https://doi.org/10.1016/j.omtm.2024.101192.

AUTHOR CONTRIBUTIONS

E.O.R. and P.C. designed research, performed research, analyzed data, and wrote paper. P.C. also provided funding to this project. C.Y. analyzed bioinformatics data and wrote paper. V.T. performed cell culture research experiments. D.Z., R.L., and A.B. performed research, generate RNAs and help with cell culture experiments. F.P.G. and K.M.C. provided project oversight. H.M.G provided input on RNA manufacturing and project oversight. E.J.S. provided input on research design, data analysis, project oversight, and provided funding to this project. D.A.M. provided input on research design, data analysis, project oversight, funding, wrote manuscript and edit manuscript.

DECLARATION OF INTERESTS

The disclosures from D.A.M. are as follows: holds patented technologies that have been licensed or have exclusive options to license to Celldex Therapeutics, Annias, Immunomic Therapeutics, and

REFERENCES

1. (2020). Center for Systems Science and Engineering (CSSE) at the (Johns Hopkins University).

2. Nasserie, T., Hittle, M., and Goodman, S.N. (2021). Assessment of the Frequency and Variety of Persistent Symptoms Among Patients With COVID-19: A Systematic Review. JAMA Netw. Open 4, e2111417. https://doi.org/10.1001/jamanetworkopen. 2021.11417.

3. Perlis, R.H., Santillana, M., Ognyanova, K., Safarpour, A., Lunz Trujillo, K., Simonson, M.D., Green, J., Quintana, A., Druckman, J., Baum, M.A., and Lazer, D. (2022). Prevalence and Correlates of Long COVID Symptoms Among US Adults. JAMA Netw. Open 5, e2238804. https://doi.org/10.1001/jamanetworkopen.2022. 38804.

4. Astuti, I., and Ysrafil. (2020). Severe Acute Respiratory Syndrome Coronavirus 2 (SARS-CoV-2): An overview of viral structure and host response. Diabetes Metab. Syndr. 14, 407–412. https://doi.org/10.1016/j.dsx.2020.04.020.

5. JHU. https://coronavirus.jhu.edu/map.html.

6. Ulrich, L., Halwe, N.J., Taddeo, A., Ebert, N., Schön, J., Devisme, C., Trüeb, B.S., Hoffmann, B., Wider, M., Fan, X., et al. (2022). Enhanced fitness of SARS-CoV-2 variant of concern Alpha but not Beta. Nature 602, 307–313. https://doi.org/10. 1038/s41586-021-04342-0.

7. Banho, C.A., Sacchetto, L., Campos, G.R.F., Bittar, C., Possebon, F.S., Ullmann, L.S., Marques, B.d.C., da Silva, G.C.D., Moraes, M.M., Parra, M.C.P., et al. (2022). Impact of SARS-CoV-2 Gamma lineage introduction and COVID-19 vaccination on the epidemiological landscape of a Brazilian city. Commun. Med. 2, 41. https://doi.org/ 10.1038/s43856-022-00108-5.

8. Tarke, A., Sidney, J., Methot, N., Yu, E.D., Zhang, Y., Dan, J.M., Goodwin, B., Rubiro, P., Sutherland, A., Wang, E., et al. (2021). Impact of SARS-CoV-2 variants on the total CD4. Cell Rep. Med. 2, 100355. https://doi.org/10.1016/j.xcrm.2021.100355.

9. CDC (2021). SARS-CoV-2 Variant Classifications and Definitions. www.cdc.gov/ coronavirus/2019-ncov/variants/variant-info.html?CDC_AA_refVal=https%3A%2F %2Fwww.cdc.gov%2Fcoronavirus%2F2019-ncov%2Fcases-updates%2Fvariant- surveillance%2Fvariant-info.html.

10. Fan, Y., Li, X., Zhang, L., Wan, S., Zhang, L., and Zhou, F. (2022). SARS-CoV-2 Omicron variant: recent progress and future perspectives. Signal Transduct. Target. Ther. 7, 141. https://doi.org/10.1038/s41392-022-00997-x.

11. Chung, Y.H., Beiss, V., Fiering, S.N., and Steinmetz, N.F. (2020). COVID-19 Vaccine Frontrunners and Their Nanotechnology Design. ACS Nano 14, 12522–12537. https://doi.org/10.1021/acsnano.0c07197.

12. Sadoff, J., Gray, G., Vandebosch, A., Cárdenas, V., Shukarev, G., Grinsztejn, B., Goepfert, P.A., Truyers, C., Fennema, H., Spiessens, B., et al. (2021). Safety and Efficacy of Single-Dose Ad26.COV2.S Vaccine against Covid-19. N. Engl. J. Med. 384, 2187–2201. https://doi.org/10.1056/NEJMoa2101544.

13. Logunov, D.Y., Dolzhikova, I.V., Zubkova, O.V., Tukhvatullin, A.I., Shcheblyakov, D.V., Dzharullaeva, A.S., Grousova, D.M., Erokhova, A.S., Kovyrshina, A.V., Botikov, A.G., et al. (2020). Safety and immunogenicity of an rAd26 and rAd5 vec- tor-based heterologous prime-boost COVID-19 vaccine in two formulations: two open, non-randomised phase 1/2 studies from Russia. Lancet 396, 887–897. https:// doi.org/10.1016/S0140-6736(20)31866-3.

14. Polack, F.P., Thomas, S.J., Kitchin, N., Absalon, J., Gurtman, A., Lockhart, S., Perez, J.L., Pérez Marc, G., Moreira, E.D., Zerbini, C., et al. (2020). Safety and Efficacy of the BNT162b2 mRNA Covid-19 Vaccine. N. Engl. J. Med. 383, 2603–2615. https://doi. org/10.1056/NEJMoa2034577.

15. Baden, L.R., El Sahly, H.M., Essink, B., Kotloff, K., Frey, S., Novak, R., Diemert, D., Spector, S.A., Rouphael, N., Creech, C.B., et al. (2021). Efficacy and Safety of the mRNA-1273 SARS-CoV-2 Vaccine. N. Engl. J. Med. 384, 403–416. https://doi.org/ 10.1056/NEJMoa2035389.

16. Alter, G., Yu, J., Liu, J., Chandrashekar, A., Borducchi, E.N., Tostanoski, L.H., McMahan, K., Jacob-Dolan, C., Martinez, D.R., Chang, A., et al. (2021). Immunogenicity of Ad26.COV2.S vaccine against SARS-CoV-2 variants in humans. Nature 596, 268–272. https://doi.org/10.1038/s41586-021-03681-2.

17. Barrett, J.R., Belij-Rammerstorfer, S., Dold, C., Ewer, K.J., Folegatti, P.M., Gilbride, C., Halkerston, R., Hill, J., Jenkin, D., Stockdale, L., et al. (2021). Phase 1/2 trial of SARS- CoV-2 vaccine ChAdOx1 nCoV-19 with a booster dose induces multifunctional anti- body responses. Nat. Med. 27, 279–288. https://doi.org/10.1038/s41591-020-01179-4.

18. Dhakal, B., Abedin, S., Fenske, T., Chhabra, S., Ledeboer, N., Hari, P., and Hamadani, M. (2021). Response to SARS-CoV-2 vaccination in patients after hematopoietic cell transplantation and CAR T-cell therapy. Blood 138, 1278–1281. https://doi.org/10. 1182/blood.2021012769.

19. Abid, M.B., Rubin, M., Ledeboer, N., Szabo, A., Longo, W., Mohan, M., Shah, N.N., Fenske, T.S., Abedin, S., Runaas, L., et al. (2022). Efficacy of a third SARS-CoV-2 mRNA vaccine dose among hematopoietic cell transplantation, CAR T cell, and BiTE recipients. Cancer Cell 40, 340–342. https://doi.org/10.1016/j.ccell.2022.02.010.

20. Piechotta, V., Mellinghoff, S.C., Hirsch, C., Brinkmann, A., Iannizzi, C., Kreuzberger, N., Adams, A., Monsef, I., Stemler, J., Cornely, O.A., et al. (2022). Effectiveness, immunogenicity, and safety of COVID-19 vaccines for individuals with hematolog- ical malignancies: a systematic review. Blood Cancer J. 12, 86. https://doi.org/10.1038/ s41408-022-00684-8.

21. Ponsford, M.J., Evans, K., Carne, E.M., and Jolles, S.; Immunodeficiency Centre for Wales and Division of Population Medicine (2022). COVID-19 Vaccine Uptake and Efficacy in a National Immunodeficiency Cohort. J. Clin. Immunol. 42, 728–731. https://doi.org/10.1007/s10875-022-01223-7.

22. Shields, A.M., Tadros, S., Al-Hakim, A., Nell, J.M., Lin, M.M.N., Chan, M., Goddard, S., Dempster, J., Dziadzio, M., Patel, S.Y., et al. (2022). Impact of vaccination on hos- pitalization and mortality from COVID-19 in patients with primary and secondary immunodeficiency: The United Kingdom experience. Front. Immunol. 13, 984376. https://doi.org/10.3389/fimmu.2022.984376.

23. Miao, L., Zhang, Y., and Huang, L. (2021). mRNA vaccine for cancer immuno- therapy. Mol. Cancer 20, 41. https://doi.org/10.1186/s12943-021-01335-5.

24. Liu, L., Liu, S., Zhang, Y., Zhou, H., Wang, Q., Tian, H., Chen, F., Qiu, H., Tang, X., Han, Y., et al. (2019). Excellent Outcomes of Allogeneic Hematopoietic Stem Cell Transplantation in Patients with Paroxysmal Nocturnal Hemoglobinuria: A Single- Center Study. Biol. Blood Marrow Transplant. 25, 1544–1549. https://doi.org/10. 1016/j.bbmt.2019.02.024.

25. Melnick, K., Dastmalchi, F., Mitchell, D., Rahman, M., and Sayour, E.J. (2022). Contemporary RNA Therapeutics for Glioblastoma. NeuroMolecular Med. 24, 8–12. https://doi.org/10.1007/s12017-021-08669-9.

26. Leen, A., Ratnayake, M., Foster, A., Heym, K., Ahmed, N., Rooney, C.M., and Gottschalk, S. (2007). Contact-activated monocytes: efficient antigen presenting cells for the stimulation of antigen-specific T cells. J. Immunother. 30, 96–107. https://doi. org/10.1097/01.cji.0000211325.30525.84.

27. Wang, G., Wang, Y., Jiang, S., Fan, W., Mo, C., Gong, W., Chen, H., He, D., Huang, J., Ou, M., and Hou, X. (2022). Comprehensive analysis of TCR repertoire of COVID-19 patients in different infected stage. Genes Genomics 44, 813–822. https://doi.org/10. 1007/s13258-022-01261-w.

28. Ogando-Rivas, E., Castillo, P., Jones, N., Trivedi, V., Drake, J., Dechkovskaia, A., Candelario, K.M., Yang, C., and Mitchell, D.A. (2022). Effects of immune checkpoint blockade on antigen-specific CD8. Microbiol. Immunol. 66, 201–211. https://doi.org/ 10.1111/1348-0421.12967.

29. Wildes, T.J., Dyson, K.A., Francis, C., Wummer, B., Yang, C., Yegorov, O., Shin, D., Grippin, A., Dean, B.D., Abraham, R., et al. (2020). Immune Escape After Adoptive T-cell Therapy for Malignant Gliomas. Clin. Cancer Res. 26, 5689–5700. https://doi. org/10.1158/1078-0432.CCR-20-1065.

30. Batich, K.A., Reap, E.A., Archer, G.E., Sanchez-Perez, L., Nair, S.K., Schmittling, R.J., Norberg, P., Xie, W., Herndon, J.E., Healy, P., et al. (2017). Long-term Survival in Glioblastoma with Cytomegalovirus pp65-Targeted Vaccination. Clin. Cancer Res. 23, 1898–1909. https://doi.org/10.1158/1078-0432.CCR-16-2057.

31. Yang, C., Dechkovskaia, A., Drake, J., Guimaraes, F., Kubilis, P., Huang, J., and Mitchell, D. (2016). Enhanced T cell activation using dendritic cells pulsed with chimeric RNAs encoding full-length LAMP-1 fusion constructs. Neuro Oncol. 18, vi93.

32. Mitchell, D.A., Batich, K.A., Gunn, M.D., Huang, M.N., Sanchez-Perez, L., Nair, S.K., Congdon, K.L., Reap, E.A., Archer, G.E., Desjardins, A., et al. (2015). Tetanus toxoid and CCL3 improve dendritic cell vaccines in mice and glioblastoma patients. Nature 519, 366–369. https://doi.org/10.1038/nature14320.

33. Nguyen, D.T., Ogando-Rivas, E., Liu, R., Wang, T., Rubin, J., Jin, L., Tao, H., Sawyer, W.W., Mendez-Gomez, H.R., Cascio, M., et al. (2022). CAR T Cell Locomotion in Solid Tumor Microenvironment. Cells 11. https://doi.org/10.3390/cells11121974.

34. Mendez-Gomez, H., DeVries, A., Castillo, P., Stover, B.D., Qdaisat, S., Von Roemeling, C., Ogando-Rivas, E., Weidert, F., McGuiness, J., Zhang, D., et al. (2023). mRNA Aggregates Harness Danger Response for Potent Cancer Immunotherapy.

35. Telenti, A., Hodcroft, E.B., and Robertson, D.L. (2022). The Evolution and Biology of SARS-CoV-2 Variants. Cold Spring Harb. Perspect. Med. 12, a041390. https://doi.org/10.1101/cshperspect.a041390.

36. Keller, M.D., Harris, K.M., Jensen-Wachspress, M.A., Kankate, V.V., Lang, H., Lazarski, C.A., Durkee-Shock, J., Lee, P.H., Chaudhry, K., Webber, K., et al. (2020). SARS-CoV-2-specific T cells are rapidly expanded for therapeutic use and target conserved regions of the membrane protein. Blood 136, 2905–2917. https://doi.org/10.1182/blood.2020008488.

37. Vasileiou, S., Kuvalekar, M., Velazquez, Y., Watanabe, A., Narula, M., Workineh, A.G., French-Kim, M., Chavez, A.T., Gilmore, S., Rooney, C.M., and Leen, A.M. (2023). Longitudinal analysis of the evolution of cellular immunity to SARS-CoV-2 induced by infection and vaccination. Haematologica 108, 1934–1939. https://doi.org/10.3324/haematol.2022.281947.

38. Vasileiou, S., Hill, L., Kuvalekar, M., Workineh, A.G., Watanabe, A., Velazquez, Y., Lulla, S., Mooney, K., Lapteva, N., Grilley, B.J., et al. (2023). Allogeneic, Off-the-Shelf, SARS-CoV-2-specific T cells (ALVR109) for the treatment of COVID-19 in high risk patients. Haematologica 108, 1840–1850. https://doi.org/10.3324/haematol.2022.281946.

39. Castillo, P., Wright, K.E., Kontoyiannis, D.P., Walsh, T., Patel, S., Chorvinsky, E., Bose, S., Hazrat, Y., Omer, B., Albert, N., et al. (2018). A New Method for Reactivating and Expanding T Cells Specific for. Mol. Ther. Methods Clin. Dev. 9, 305–312. https://doi.org/10.1016/j.omtm.2018.03.003.

40. Melenhorst, J.J., Castillo, P., Hanley, P.J., Keller, M.D., Krance, R.A., Margolin, J., Leen, A.M., Heslop, H.E., Barrett, A.J., Rooney, C.M., and Bollard, C.M. (2015). Graft versus leukemia response without graft-versus-host disease elicited by adoptively transferred multivirus-specific T-cells. Mol. Ther. 23, 179–183. https://doi.org/10.1038/mt.2014.192.

41. Kennedy-Nasser, A.A., Ku, S., Castillo-Caro, P., Hazrat, Y., Wu, M.F., Liu, H., Melenhorst, J., Barrett, A.J., Ito, S., Foster, A., et al. (2014). Ultra low-dose IL-2 for GVHD prophylaxis after allogeneic hematopoietic stem cell transplantation mediates expansion of regulatory T cells without diminishing antiviral and antileukemic activity. Clin. Cancer Res. 20, 2215–2225. https://doi.org/10.1158/1078-0432.CCR-13-3205.

42. Kusnadi, A., Ramírez-Suástegui, C., Fajardo, V., Chee, S.J., Meckiff, B.J., Simon, H., Pelosi, E., Seumois, G., Ay, F., Vijayanand, P., and Ottensmeier, C.H. (2021). Severely ill COVID-19 patients display impaired exhaustion features in SARS-CoV-2-reactive CD8. Sci. Immunol. 6, eabe4782. https://doi.org/10.1126/sciimmunol.abe4782.

43. Snyder, T.M., Gittelman, R.M., Klinger, M., May, D.H., Osborne, E.J., Taniguchi, R., Zahid, H.J., Kaplan, I.M., Dines, J.N., Noakes, M.T., et al. (2020). Magnitude and Dynamics of the T-Cell Response to SARS-CoV-2 Infection at Both Individual and Population Levels. Preprint at medRxiv. https://doi.org/10.1101/2020.07.31.20165647.

44. Klinger, M., Pepin, F., Wilkins, J., Asbury, T., Wittkop, T., Zheng, J., Moorhead, M., and Faham, M. (2015). Multiplex Identification of Antigen-Specific T Cell Receptors Using a Combination of Immune Assays and Immune Receptor Sequencing. PLoS One 10, e0141561. https://doi.org/10.1371/journal.pone.0141561.

45. Fang, S., Liu, S., Shen, J., Lu, A.Z., Wang, A.K.Y., Zhang, Y., Li, K., Liu, J., Yang, L., Hu, C.D., and Wan, J. (2021). Updated SARS-CoV-2 single nucleotide variants and mortality association. J. Med. Virol. 93, 6525–6534. https://doi.org/10.1002/jmv.27191.

46. Pablo, R.G.J., Roberto, D.P., Victor, S.U., Isabel, G.R., Paul, C., and Elizabeth, O.R. (2021). Big data in the healthcare system: a synergy with artificial intelligence and blockchain technology. J. Integr. Bioinform. 19, 20200035. https://doi.org/10.1515/jib-2020-0035.

47. Yang, C., Tian, G., Dajac, M., Doty, A., Wang, S., Lee, J.H., Rahman, M., Huang, J., Reynolds, B.A., Sarkisian, M.R., et al. (2022). Slow-Cycling Cells in Glioblastoma: A Specific Population in the Cellular Mosaic of Cancer Stem Cells. Cancers 14, 1126. https://doi.org/10.3390/cancers14051126.

48. Quinlan, A.R., and Hall, I.M. (2010). BEDTools: a flexible suite of utilities for comparing genomic features. Bioinformatics 26, 841–842. https://doi.org/10.1093/bioinformatics/btq033.